Mechanically Strong Double Network Photocrosslinked Hydrogels from *N, N*-Dimethylacrylamide and Glycidyl Methacrylated Hyaluronan

Lihui Weng[1], **Andrew Gouldstone**[2], **Yuhong Wu**[2], and **Weiliam Chen**[1,*]

1 *Department of Biomedical Engineering, State University of New York at Stony Brook, Stony brook, NY 11794-8181*

2 *Department of Materials Science and Engineering, State University of New York at Stony Brook, Stony Brook, NY 11794-2275*

Abstract

Hyaluronan (HA) is a natural polysaccharide abundant in biological tissues and it can be modified to prepare biomaterials. In this work, HA modified with glycidyl methacrylate was photocrosslinked to form the first network (PHA), and then a series of highly porous PHA/*N, N*-dimethylacrylamide (DAAm) hydrogels (PHA/DAAm) with high mechanical strength were obtained by incorporating a second network of photocrosslinked DAAm into PHA network. Due to synergistic effect produced by double network (DN) structure, despite containing 90% of water, the resulting PHA/DAAm hydrogel showed a compressive modulus and a fracture stress over 0.5 MPa and 5.2 MPa, respectively. Compared to the photocrosslinked hyaluronan single network hydrogel, which is generally very brittle and fractures easily, the PHA/DAAm hydrogels are ductile. Mouse dermal fibroblast was used as a model cell line to validate *in vitro* non-cytotoxicity of the PHA/DAAm hydrogels. Cells deposited extracellular matrix on the surface of these hydrogels and this was confirmed by positive staining of Type I collagen by Sirius Red. The PHA/DAAm hydrogels were also resistant to biodegradation and largely retained their excellent mechanical properties even after two months of co-culturing with fibroblasts.

Keywords

Hyaluronan; *N, N*-dimethylacrylamide; Hydrogels; Photocrosslinkable; Double network

1. Introduction

Tissue engineering technology has shown great promises in producing functional replacements for diseased tissues and organs including skin [1], heart valve leaflets [2], and as spinal disc replacements [3]. Hydrogel is a class of three dimensional crosslinked polymeric materials with unique properties (such as swelling, water retention, tissue mimetic, etc.) appealing for

* Corresponding author: Weiliam Chen, Department of Biomedical Engineering, State University of New York-Stony Brook, Stony Brook, NY11794-8181, Tel: 631-444-2788, Fax: 631-444-6646, Email: weiliam.chen@stonybrook.edu.

tissue engineering. The structural integrity and physicochemical properties of hydrogels could be modulated by crosslinking density and material combinations [4].

Hyaluronan (HA), a natural glycosaminoglycan, composed of β-1,4-linked units of β-1,3-linked glucuronic acid and *N*-acetyl-D-gucosamine, is an abundant component in connective, epithelial, and neural tissues [5]. HA is a major component of extracellular matrix (ECM) that contributes significantly to cell proliferation and growth [6], and it also mediates early inflammatory response crucial for wound healing. HA based materials offer great advantages including biocompatibility and versatility in producing materials with a broad range of properties. A number of techniques have been developed to modify and crosslink HA via its carboxylic and hydroxyl groups while retaining the crucial biological properties, including using dihydrazide [7,8], carbodiimides [9,10], dialdehyde [11,12], disulfide [5,13] and a variety of other agents [14–18]. Biodegradable hydrogels fabricated from photocrosslinking glycidyl methacrylate (GMA) derivatized HA (MeHA) are non-cytotoxic with retained intrinsic biological activity for promoting endothelial cell proliferation [19]. In addition, as reported by Setton et al [20], articular chondrocytes were successfully encapsulated in photo-polymerizable HA hydrogel *in vivo*, with no adverse effects.

Although the photocrosslinked MeHA hydrogel is highly biocompatible, it is brittle. This lack of structural integrity largely limits its potential in many fields where good mechanical properties are required. Integrating a synthetic polymer into the MeHA hydrogel matrix is one possible strategy to enhance its mechanical properties. Due to its exceptional biocompatibility, the hydrophilic synthetic polymer poly (*N*, *N*-dimethylacrylamide) (PDMAAm) has been widely utilized in the biomedical fields [21,22]. Moreover, grafting of the *N*, *N*-dimethylacrylamide (DMAAm) monomer onto substrates like poly(dimethylsiloxane) produces a material with unique properties suitable for determining the diffusion characteristics of small molecule drugs, glucose, insulin, and albumin *in vitro* [23].

In this study, we reported the synthesis of hydrogels composed of interpenetrating double networks (DN) by combining HA with PDMAAm. Methyacrylate groups were first introduced onto HA chains and photocrosslinked to prepare the first hydrogel network (photocrosslinked hyaluronan, PHA). The second network PDMAAm subsequently formed by photocrosslinking of *N*, *N*-dimethylacrylamide in the presence of the first formed HA network (i.e., PHA/DAAM). This DN structure resulted in a series of hydrogels with exceptional mechanical performance. Structure and physical properties of the resulting hydrogels were investigated by SEM, swelling and compression tests. Mouse dermal fibroblast was used as an *in vitro* model to evaluate the initial non-cytotoxicity of these hydrogels; deposition of ECM on the three-dimensional network was also assessed. The results showed that the hydrogels were both mechanically strong and non-cytotoxic, and thus have many potential biomedical applications including implantables designed for load bearing.

2. Materials and methods

2.1 Materials

Sodium hyaluronan (M_{w}, 1.5×10^6) was provided by Engelhard, Inc. (now, BASF) (Stony Brook, NY). Glycidyl methacrylate (GMA), *N*, *N*-Dimethylacrylamide (DAAm), *N*, *N'*-methylene bisacrylamide (MBAAm) triethylamine (TEA), tetrabutylammonium bromide (TBAB), α-ketoglutaric acid, and Sirius Red were purchased from Sigma-Aldrich Company (St Louis, MO).

Cell culture inserts (polycarbonate, 6.5 mm diameter, 0.2 μm pore size) were obtained from NUNC (Rochester, NY, USA). M. DUNNI (clone III8C) murine dermal fibroblast CRL-2017 and McCoy's 5A medium were obtained from ATCC (Manassas, VA, USA). Fetal Bovine

Serum (FBS) was acquired from Hyclone (Logan, UT, USA) and Penicillin-Streptomycin (Pen-Strep) solution was obtained from Gibco (Grand Island, NY, USA). MTS assay kit (CellTiter 96s) was purchased from Promega (Madison, WI). All other chemicals were of reagent grade and deionized distilled water was used.

2.2 Synthesis of photocrosslinkable HA

Photocrosslinkable HA was synthesized by derivatizing HA with methacrylate following a method described previously [19]. Briefly, into 1% g/mL HA aqueous solution, 20 mol-% TEA (relative to the total hydroxyls on HA), 20 mol% TBAB, and 20 fold excess of GMA were added separately and thoroughly mixed; the reaction was carried out at room temperature for 24 h. The reaction mixture was then dialyzed extensively against 0.1 M NaCl followed by water. The final photocrosslinkable HA was recovered after lyophilization. The substitution degree of HA was determined by ^{1}H-NMR (Varian Unity-500, CA, USA).

2.3 Preparation of the photocrosslinked hyaluronan (PHA) hydrogel

The PHA hydrogel was prepared by irradiating a 2% (w/v) GMA derivatized HA solution with UV light at 365 nm (Fisher company, Hampton, NH, USA) for 2 hours in the presence of a photo-initiator 2-oxo-ketoglutaric acid, at a concentration of 0.1 mol-%.

2.4 Preparation of double network (PHA/DAAM) hydrogels

A series of PHA/DAAM hydrogels with incremental properties were prepared. For a typical preparation, a previously formed PHA hydrogel was first immersed in a DAAm solution at ambient temperature, where the concentrations of DAAm monomers used were 1, 2, 3, 4, and 5 mol/L. Moreover, these DAAm solutions contained various amounts of MBAAm crosslinker (0, 0.01, 0.05, 0.1, 0.5, 1, and 2 mol-% with respect to the DAAm monomer concentration) as well as a photoinitiator at 0.1 mol-%. Upon equilibrating of the PHA hydrogel with the DAAm monomers solution, a second network was formed in the presence of the first network by irradiating the DAAm equilibrated PHA hydrogel for 2 hours under UV light at 365 nm. The hydrogel formed was referred as PHA/D-x-y (x is the monomer concentration, whereas, y is the crosslinker concentration). For example, a hydrogel prepared from a PHA network combined with a second network formed with 3 mol/L DAAm, 0.01 mol-% MBAAm and 0.1 mol-% 2-oxoglutaric acid, was coded as PHA/D-3-0.01.

2.5 Scanning electronic microscopy

The PHA/DAAM hydrogels were snap frozen using liquid nitrogen followed by lyophilization. Fractured pieces with dimensions ~5 mm × 2 mm × 3 mm were mounted onto an aluminum board with copper tape and sputter-coated with gold. The surface and cross-sections were examined with a field-emission scanning electron microscope (SFEG Leo 1550, AMO GmbH, Aachen, Germany) at 20 kV.

2.6 Equilibrium water uptake measurements

Equilibrium swelling studies were performed on PHA/DAAM hydrogels. Lyophilized hydrogels were first weighed (W_d) and immersed in 0.01 M PBS at 37 °C. After five days of equilibration, the hydrogels were removed from the PBS solution, blotted with tissue for removal of excess water, and weighed (W_s) again. The equilibrium water content (EWC) was calculated through the following equation:

$$EWC(\%)=100(W_s - W_d)/W_s. \tag{1}$$

For comparison, the equilibrium water uptake studies were also performed on both single network PHA and PDAAm hydrogels, respectively.

2.7 Mechanical properties of the PHA/DAAM hydrogel

Mechanical properties of the swollen hydrogels before and after 2-month of incubation with cell culture were performed with a screw-driven desktop loading frame (Model 1K-16 Universal Materials Tester, Interactive Instruments, USA). A cylindrical hydrogel specimen (diameter: 8 mm, height: 5 mm) was set on the lower plate and compressed by the upper plate connected to a load cell, with an applied strain rate set at 0.1% per min at ambient temperature. The initial compressive modulus was determined by the average slope in a range of 0–10% strain from the stress-strain curve. The fracture stress was determined from the peak of the stress-strain curve. To evaluate the changes in mechanical properties of the hydrogels subject to cell degradation, co-culture was performed using as a model cell line M. DUNNI mouse dermal fibroblast CRL-2017 cells cultured in McCoy's 5A medium containing 10% FBS and 1% Pen-Strep solution maintained at 37 °C under a humidified atmosphere of 5% CO_2. Briefly, hydrogel cylinders (diameter: 8 mm, height: 5 mm) were deposited in 24 well plates, and 1×10^6 cells were then seeded in each well. The medium was changed every other day. After 2 month of cell culture, the hydrogel cylinders were retrieved and fixed with 70% ethanol, followed by rinsing three times with PBS, and maintained in PBS for mechanical testing.

2.8 Cytotoxicity

Cell toxicity assay was carried out with same cell line on representative hydrogels (PHA, PHA/D-3-0.01, PHA/D-3-0.05, and PHA/D-3-2) in 96-well plates (1×10^5 cells/mL). To avoid the error caused by removing the hydrogel pieces each time while performing the assay, a non-contact methodology was employed to evaluate the cytotoxicity of the PHA/DAAM hydrogels. Briefly, sterilized PHA and PHA/DAAM hydrogel pieces, tailored to 5 mm × 2 mm × 2 mm, were first deposited in culture inserts and immersed in cell-seeded culture wells (n = 3 per group). Cell viability was determined by MTS assay on day 0, 3, 7, 10 and 14. For each time point, 20 μL MTS solution were added to the culture medium, and monolayer cultured cells were used as controls. After incubating at 37 °C for 1 h, the absorbance of solutions were determined at 490 nm.

2.9. Long-term co-culture with fibroblasts and ECM deposition on the surface of PHA/DAAM hydrogel

Long-term cell culture was performed on the PHA/DAAM hydrogels in 48-well plates to determine the changes in hydrogel morphology and ECM deposition on the surface of the hydrogel. A piece of hydrogel (approximate dimension: 6 mm × 6 mm ×1 mm) was deposited in each well, 1×10^5 cells were then seeded directly. The medium was changed every other day. To observe cell morphology on the surface of PHA/DAAM hydrogels, images of cells were acquired *in situ* with a QCapture 5 imaging software (Surrey, Canada). After cultured with mouse fibroblast in a direct contact mode for 1 month, the PHA/DAAM hydrogels were retrieved and fixed with 70% ethanol for 30 min, rinsed gently with PBS followed by distilled water. To evaluate the extracellular matrix (ECM) deposition on the surface of the hydrogels, the collagen secreted was detected with Picrosirius Red (0.1% Sirius Red in saturated picric acid) staining [24]. Initially, a regular bright field image was obtained as control. The hydrogel appears yellow and extracellular matrix deposited appears red. Under polarized light, an image from the same region of the hydrogel surface was captured to evaluate collagen deposition. The collagen in the extracellular matrix appears as bright red or yellow, while the hydrogel was dark. SEM was also performed on the hydrogel lyophilized after co-culturing with fibroblast to corroborate with the results obtained by polarization microscopy.

2.10 Statistical analysis

Statistical analysis was performed using a Student's t-test with a $q<0.05$ for statistical significance. All values are reported as the mean and standard error of mean.

3. Results and Discussion

3.1. Synthesis of PA and hydrogel formation

Introducing methyacrylate groups onto HA is a facile technique to produce a photocrosslinkable MeHA macromer. In this work, the reaction condition of HA derviatization with GMA was chosen according to Schmidt's report [19], where the reaction occurred by a trans-esterification mechanism. Fig. 1 shows the ^{1}H NMR spectra of modified HA and native HA as control. Compared to native HA, modified HA showed two new peaks at ~5.6 and ~6.1 ppm attributable to the presence of acrylate groups on HA, confirming grafting of methyacrylate groups on HA chain, which was consistent with the published results [19]. The methyacrylation percentage of HA was determined by integrating the methyl peak at 1.9 ppm and the acrylic double bond peaks, and the result suggested approximately 10% modification.

In the presence of a photo-initiator, the methyacrylate HA macromer, when exposed to UV light, undergoes a free radical polymerization to form a three-dimensional crosslinked hydrogel (PHA). The PHA hydrogel formed was then immersed in an aqueous DAAm solution containing various amounts and combinations of crosslinker and photo-initiator until equilibrium was reached, respectively. This was followed by subsequent exposure to UV for polymerization of the DAAm entrapped in the swollen PHA hydrogel, leading to formation of a double network hydrogel.

3.2. Morphology of the PHA/DAAm hydrogels

Fig. 2 depicts representative SEM images of the cross-section for lyophilized PHA (A), PHA/D-3-0.01 (B), PHA/D-3-0.05(C), and PHA/D-3-2 (D) hydrogels. All hydrogels were highly porous throughout the cross-section. Pure PHA hydrogel exhibited the largest pore size (average: 50 μm) among the four hydrogel formulations. Due to the presence of the second PDAAm network, which increased the relative crosslinking density of the hydrogel structure, the other three hydrogels PHA/D-3-0.01, PHA/D-3-0.05, and PHA/D-3-2 appeared to have more compact porous structures with an average pore size ranging from 10 to 20 μm. Evidently, due to the higher crosslinking density, the pore partitions of PHA/D-3-2 hydrogel were the thickest.

3.3 Equilibrium water content (EWC) in hydrogels

Fig. 3A and 3B depict the relationship between EWCs of PHA/DAAm hydrogels and concentrations of monomer and crosslinkers used, respectively. All hydrogels exhibited EWCs value greater than 80%. In Fig. 3A, the EWC of pure PHA hydrogel, as a control (i.e., DAAm monomer concentration = 0 mol/L), was approximately 98%. Upon introducing the second network, the EWC values of the PHA/DAAm hydrogel formulations decreased from 98% to 88%, attributable to an increase in the crosslinking density, with a corresponding increase of the DAAm monomer concentration from 0 to 5 mol/L, while maintaining the crosslinker concentration at 0.1 mol-%. These results were in a good agreement with those reported previously [25, 26]. Baker et al [27] suggested that the strong dependence of acrylamide hydrogels swelling behavior on initial monomer concentrations was a reflection of increasing network-chain interpenetration with rising monomer concentration. Haraguchi et al [26] also proposed that a higher initial DAAm content in hydrogels would increase effective crosslinking density. Thus, the observed inverse correlation of swelling with monomer concentration was expected. Moreover, the EWC result was also dependent on the crosslinker concentration of MBAAm in the second network, as depicted in Fig. 3B. A decrease in EWC was observed with an increase in the concentration of crosslinker in the second network. For example, when the concentration of DAAm monomer was kept at 3 M, an increase in MBAAm concentration from 0.01 mol-% to 2 mol-% reduced the EWC from 94% to 83%. Higher crosslinker concentration created a denser polymer network and thus rendered the polymeric chains to

move in closer proximity to each other, which enabled stronger hydrophobic interactions leading to lower EWC [28].

3.4. Mechanical properties of the hydrogel

Fig. 4 depicts the stress-strain behavior of PHA, PHA/D-3-0.05, and D-3-0.05 hydrogels under uniaxial compression. Pure PHA and D-3-0.05 single network hydrogels fractured at stresses 0.29 MPa and 0.04 MPa, respectively, while the PHA/D-3-0.05 possessed a fracture stress of over 5.25 MPa. The fracture strain of PHA/D-3-0.05 hydrogel was 87.1%, which was considerably higher than that of either the PHA (56.1%) hydrogel or the D-3-0.05 (78.4%) hydrogel. The mechanical effect produced by a DN structure [29,30] suggested that one of the networks contributed to the elastic stress, whilst the other one contributed to the strain. The stress-strain profiles obtained indicated that the PHA hydrogel was brittle whilst the D-3-0.05 hydrogel was more ductile. Therefore, it could be inferred that the brittle PHA network in PHA/D-3-0.05 contributed to the elastic stress and the D-3-0.05 network contributed to the strain of the double network hydrogel.

The initial compressive moduli of hydrogels were deduced from the stress-strain profiles. All PHA/DAAm hydrogels showed similar initial compressive moduli of order 0.1 MPa. Representative results of the initial compressive moduli of PHA, PHA/D-3-0.01, PHA/D-3-0.05, and PHA/D-3-2 hydrogels are summarized in Table 1. With the exception of the PHA hydrogel possessing a relatively low compressive modulus at 0.045 MPa, the other three hydrogels exhibited comparable moduli in the range of 0.3–0.6 MPa, indicating a higher crosslinking for PHA/DAAm hydrogel [31]. The compressive moduli of the hydrogels after 2 months of cell culture are also presented in Table 1. Fibroblast secretes a myriad of hydrolases, including hyaluronidase [32], which is capable of degrading the PHA network despite photocrosslinking. Evidently, the moduli of PHA and PHA/DAAm hydrogels all declined after 2 months, with the comparable final moduli of all formulations (the single network PHA hydrogel as the control). However, as summarized in Fig. 5, the fracture stresses varied considerably among the hydrogels. Fig. 5A shows the effect of varying DAAm monomer concentration on the fracture stress of the PHA/DAAm hydrogels. Increasing the DAAm concentration from 0 to 3 mol/L resulted in a gradual enhancement of the fracture stress of the hydrogels from 0.29 to 4.12 MPa, further increase in DAAm concentration led to a gradual decline in the fracture stress of hydrogels. In particular, a double network system, containing one stiff but brittle first network and one soft but ductile second network, typically exhibit excellent overall mechanical properties in both strength and toughness [29]. This aspect is distinctively different from common interpenetrating polymer hydrogel networks where the resultant mechanical properties represent an average of those of the two individual networks [33,34]. Two crucial structural parameters affect the properties of DN hydrogels, i.e. the molar ratio of the second to the first network and the crosslinking density of the second network. There is an optimal value for both the molar ratio and the crosslinking density for the first network to reach a stiff and brittle state and for the second network to be both soft and ductile, respectively. Apparently, the DAAm concentration of 3 mol/L was optimal for achieving the highest mechanical strength for PHA/DAAm hydrogel formulations at a crosslinker concentration of 0.1 mol-%. The effect of the crosslinker concentration on the mechanical properties of the hydrogel was examined while maintaining the DAAm monomer concentration at 3 mol/L (Fig. 5B). Due to the DN structure, the fracture stress attained a maximum value of 5.25 MPa at a crosslinker concentration of 0.05 mol-%. For the PHA/D-3-0.05 hydrogel, the abrupt increase in the mechanical strength likely did not result from an increase in chemical crosslinkage or physical entanglement since the second network was loosely crosslinked. DN effect suggests that the highly crosslinked first network has a relatively higher modulus but rather brittle (see Fig. 4). Under compression, stress could easily develop locally inside the network, leading to formation of cracks. However, the presence of the soft but loosely

crosslinked second network could effectively dissipate the stress imposed during compression by deforming the network conformation and/or sliding the physical entanglement points along the polymer chains [29]. As shown in Fig. 5B, increasing the crosslinker concentration from 0.05 to 2 mol-% resulted in a progressive decrease of fracture stress of the hydrogels. This increase in the crosslinker concentration resulted in substantial increase in the crosslinking density and thus, formation of a stiffer network with very limited capacity to dissipate stress imposed during compression, leading to the reversal of the DN effect.

In Fig. 4B, the water content of the PHA/DAAm hydrogel prepared from 3 mol/L of DAAm with a 0.05 mol-% crosslinker concentration was greater than 93%. In general, when hydrogels are fully swollen, their compressive fracture stresses are lowered due to the softer network. Remarkably, the fully swollen PHA/D-3-0.05 hydrogel still possessed a high fracture stress at 5.25 MPa, implying that the DN structure could greatly improve the mechanical strength of the swollen hydrogels. Moreover, these hydrogels composed of double networks all exhibited one definitive fracture line when broke (see Fig. 5a); this pattern was distinctively different from hydrogels composed of a single network or interpenetrating polymer networks without the DN effect; they tended to fracture into multiple fragments under compression (Fig. 5b).

For comparison, the fracture tests were also performed on the PHA/DAAm hydrogels after 2 months of incubation in cell culture. There was no noticeable change on shape of these hydrogel specimens when compared to their pristine counterparts by gross observation. As shown in Fig. 5 (circles), all PHA/DAAm hydrogels consistently displayed decreased failure stress after co-cultured with cells. The fracture stress of PHA single network hydrogel decreased drastically from 0.29 MPa to 0.019 MPa (Fig. 5A), whereas the fracture stress of PHA/DAAm hydrogels were moderately reduced by cell-mediated degradation. Furthermore, the peak value (i.e., the DN effect) was maintained at a MBAAm concentration of 0.05 mol-% (Fig. 5B). The result was consistent with the resistance of DAAm networks to biodegradation. Hydrogels with higher DAAm or MBAAm concentrations exhibited less decrease in failure stress.

3.5. Cytotoxicity analyses and in vitro resistance of biodegradation

The cytotoxicity potential of PHA/DAAm hydrogels was evaluated by co-culturing dermal fibroblasts for 2 weeks utilizing an indirect contact method; cell viabilities were determined by MTS assay at 3, 7, 10 and 14 days. The hydrogels were deposited in cell culture inserts to avoid the disturbance of cells anchored to the culture wells during their removal for assay.

Both the morphology and the amount of cells seeded in all wells, during the entire culture span, did not show noticeable difference (data not shown). Fig. 6 depicted the results of MTS assay for PHA/D-3-0.01 (Gel 1), PHA/D-3-0.05 (Gel 2), PHA/D-3-2 (Gel 3), and PHA (Gel 4). After 3 days of incubation, the absorbance of all samples increased considerably with no significant difference among all groups. The presence of hydrogels did not affect cell growth and thus, validating the hydrogels' lack of cytotoxicity. In general, the media's absorbance increased steadily from 0 to 14 days with values comparable to those of their corresponding controls indicating that the presence of PHA/DAAm hydrogels did not affect cell proliferation. Varying the concentration of either DAAm monomer (from 0 to 3 mol/L) or the crosslinker (from 0.01 to 2 mol-%) for hydrogel preparation did not show any noticeable effect on cell growth. Moreover, as mentioned previously, after prolonged co-culturing with cells, the hydrogel did not exhibit drastic change in their shapes or mechanical properties, suggesting that they were not easily degraded by cells. This could be attributed to the facts that the stable bonds formed by free radical polymerization were highly resistant to biodegradation, and the poly (*N*, *N*-dimethyacrylamide) hydrogel is a non-biodegradable material.

3.6 Organization and morphology of cells on PHA/DAAm hydrogel surface and ECM production

The morphology of cells deposited directly on hydrogels was monitored continuously for 1 month. Fig. 7 depicted representative images of the fibroblasts on the surface and on the en face side of PHA/D-3-0.01 (A, B) and PHA/D-3-0.05 (C, D) hydrogels. Cells assumed round morphology initially and tended to cluster (marked with " ♠ ") suggesting that the surfaces of pristine PHA/DAAm hydrogels were not conducive to cell attachment (Fig. 7A and C). Similar cellular behavior was previously reported by on the interaction of fibroblast cells and polymer surface Tamada et al. [35]. At the very beginning, cells deposited on hydrogel surface could be detached by vigorous rinsing (data not shown), most likely due to lack of firm anchoring of cells on the hydogels. This observation was in good agreement with previously published data suggested that both HA and PDAAm did not form conducive surface for cell attachment [5, 36]. Thus, the PHA/DAAm hydrogels were not expected to form a favorable environment for cell attachment. Spreading of fibroblasts on polymer surfaces is dependent on the polar surface free energy; the extent of cell spreading is low when the polar surface free energy is less than 5 erg/cm^2 [37]. Therefore, the low polar surface free energy of the hydrogel surface could possibly account for the poor cell spreading. However, fibroblasts readily attached to the side faces of the hydrogel (see Fig. 7B and D) and formed cluster similar to that on the hydrogel surface. An increase in the surface roughness of polymer could enhance the cell adhesion strength [38], and thus, the ready attachment of cells to the side faces could be attributed to its roughness created by cutting. Nonetheless, cells appeared to firmly adhere to the hydrogel after one month of incubation, and some of the cells in the cell cluster started to spread out to some extent (see Fig. 7C). It could be postulated that fibroblasts began to secret ECM once deposited on the PHA/DAAm hydrogel surface creating an environment conducive to their attachment.

Cells are known to deposit ECM on biomaterial surfaces and ECM is essential in regulating cellular behavior [39]. Collagen is the major protein comprising the ECM; therefore, the presence of collagen is indicative of ECM production. PHA/DAAm hydrogels were co-cultured with fibroblasts for 1 month and subjected to Sirius Red staining in order to confirm the presence of collagen. Fig. 8 shows the surface of PHA/D-3-0.01 (A, B) and PHA/D-3-0.05 (C, D) hydrogels after staining. They were observed with both conventional and polarized light under bright field; under conventional light, besides collagen, depositions of other ECM ingredients showed up. Stained and observed under a polarized light, portions of collagen fibers showed the characteristic birefringence (Fig. 8B, and D). It is reported that type I collagen appeared as reddish-yellow, and type III collagen appeared to be greenish under polarized light [40]. Apparently, the collagen deposited on the PHA/DAAm hydrogels was mostly of Type I. There was no noticeable difference in collagen compositions among the ECMs deposited on the surfaces of all PHA/DAAm hydrogel formulations. Therefore, despite their lack of initial attachment, fibroblasts gradually produced and deposited ECM on hydrogel surface.

Fig. 9 showed the representative morphology of the fibroblasts underneath the PHA/D-3-0.05 hydrogels after one week (Fig. 9A), 2 week (Fig. 9B), and 1-month (Fig. 9C) of incubation, respectively. Fig. 9B was captured in the presence of an intact piece of hydrogel (right side). There was no morphological difference between the fibroblasts residing underneath the hydrogel or on the culture dish (left side, Fig. 9B), suggesting that the hydrogel does not have adverse effect on the fibroblasts. Cell underneath the hydrogel continued to proliferate (Fig 9. C) after 2 week, which further demonstrated the lack of cytotoxicity of the hydrogels.

Hydrogels co-cultured with fibroblasts were lyophilized and examined under SEM to corroborate with the ECM staining results obtained. Representative SEM images of the PHA/D-3-0.05 hydrogels were shown in Fig. 10. Uneven morphology was observed (Fig. 10A) on the pristine hydrogel surface (i.e., never co-cultured with cells), which was generally ridden with multi-holes or crumples (Fig. 10A). After 1 month of co-culturing with fibroblasts, ECM

appeared to have accumulated on the surface of the hydrogel (Fig. 10B, marked with "♠"). As shown in Fig. 10B, the hydrogel surface was almost completely masked by ECM with a partially covered area where the porous hydrogel structure remained visible. The uncovered part of surfaces maintained similar morphology as their pristine counterparts as shown in Fig. 10A.

4. Conclusions

Double network hydrogels based on HA and poly (*N, N*-dimethylacrylamide) have been prepared by a two-step photocrosslinking process. The hydrogels exhibit porous internal structures with good swelling properties. Their mechanical properties are related to both the DAAm monomer concentration and the crosslinker concentration of the second network. Due to the synergistic effect of DN structure, the new hydrogels possess greatly enhanced mechanical properties as compared to the single network PHA hydrogel; the loosely crosslinked second network dissipates stress during compression contributing to the high mechanical strength of the double network hydrogel. Even though the PHA/DAAm hydrogel contains more than 90% water, its fracture stress is as high as 5.2 MPa. The PHA/DAAm hydrogels are non-cytotoxic but highly resistant to biodegradation and they largely retain their excellent mechanical properties even after 2 months of co-culturing with fibroblasts. The results of long-term cell culture reveals that fibroblasts secrete ECM (mostly Type I collagen) to modify the surface of the hydrogels. The collective performance profile of the PHA/DAAm hydrogels strongly suggests that this class of material has great potential for biomedical applications, particularly those designed for load bearing; future investigation will direct at exploring its potential as spinal disc substitutes.

Acknowledgements

References

1. Boucard N, Viton C, Agay D, Mari E, Roger T, Chancerelle Y, Domard A. The use of physical hydrogels of chitosan for skin regeneration following third-degree burns. Biomaterials 2007;28:3478–88. [PubMed: 17482258]

2. Sodian R, Sperling JS, Martin DP, Egozy A, Stock U, Mayer JE Jr, Vacanti JP. Fabrication of a trileaflet heart valve scaffold from a polyhydroxyalkanoate biopolyester for use in tissue engineering. Tissue Eng 2000;6:183–8. [PubMed: 10941212]

3. Bono CM, Garfin SR. History and evolution of disc replacement. The Spine J 2004;4:145S–50S.

4. Drury JL, Mooney DJ. Hydrogels for tissue engineering: Scaffold design variables and applications. Biomaterials 2003;24:4337–51. [PubMed: 12922147]

5. Shu XZ, Liu YC, Palumbo F, Prestwich GD. Disulfide-crosslinked hydaluroan-gelatin hydrogel films: a covalent mimic of the extracelluar matrix for *in vitro* cell growth. Biomaterials 2003;24:3825–34. [PubMed: 12818555]

6. Joddar B, Ramamurthi A. Fragment size- and dose-specific effects of hyaluronan on matrix synthesis by vascular smooth muscle cells. Biomaterials 2006;27:2994–3004. [PubMed: 16457881]

7. Yeo Y, Bellas E, Highley CB, Langer R, Kohane DS. Peritoneal adhesion prevention with an in situ cross-linkable hyaluronan gel containing tissue-type plasminogen activator in a rabbit repeated-injury model. Biomaterials 2007;28:3704–13. [PubMed: 17512979]

8. Jia X, Colombo G, Padera R, Langer R, Kohane DS. Prolongation of sciatic nerve blockade by in situ cross-linked hyaluronic acid. Biomaterials 2004;25:4797–804. [PubMed: 15120526]

9. Park SN, Lee HJ, Lee KH, Suh H. Biological characterization of EDC-crosslinked collagen –hyaluronic acid matrix in dermal tissue restoration. Biomaterials 2003;24:1631–41. [PubMed: 12559823]

10. Chang CH, Kuo TF, Lin CC, Chou CH, Chen KH, Lin FH, Liu HC. Tissue engineering-based cartilage repair with allogenous chondrocytes and gelatin–chondroitin–hyaluronan tri-copolymer scaffold: A porcine model assessed at 18, 24, and 36 weeks. Biomaterials 2006;27:1876–88. [PubMed: 16278014]

11. Tomihata KJ, Ikada Y. Crosslinking of hyaluronic acid with glutaraldehyde. J Polym Sci: Part A: Polym Chem 1997;35:3553–9.

12. Bulpitt P, Aeschliman D. New strategy for chemical modification of hyaluronic acid: Preparation of functionized derivatives and their use in the formation of novel biocompatible hydrogels. J Biomed Mater Res 1999;47:152–69. [PubMed: 10449626]

13. Liu Y, Shu XZ, Gray SD, Prestwich GD. Disulfide-crosslinked hyaluronan–gelatin sponge: Growth of fibrous tissue *in vivo*. J Biomed Mater Res A 2004;68:142–9. [PubMed: 14661259]

14. Segura T, Anderson BC, Chung PH, Webber RE, Shull KR, Shea LD. Crosslinked hyaluronic acid hydrogels: A strategy to functionalize and pattern. Biomaterials 2005;26:359–71. [PubMed: 15275810]

15. Balazs, EA.; Leshchiner, A. Crosslinked gels of hyaluronic acid and products containing such gels. 1986. United States Patent No. 4,582,865

16. Dulong V, Lack S, Cerf DL, Picton L, Vannier JP, Muller G. Hyaluronan-based hydrogels particles prepared by crosslinking with trisodium trimetaphosphate. Synthesis and characterization. Carbohydr Polym 2004;57:1–6.

17. Ramamurthi A, Vesely I. Ultraviolet light-induced modification of crosslinked hyaluronan gels. J Biomed Mater Res A 2003;66:317–29. [PubMed: 12889002]

18. Burdick JA, Chung C, Jia XQ, Randolph MA, Langer R. Controlled degradation and mechanical behavior of photopolymerized hyaluronic acid networks. Biomacromolecules 2005;6:386–91. [PubMed: 15638543]

19. Leach JB, Bivens KA, Patrick CW Jr, Schmidt CE. Photocrosslinked hyaluronic acid, hydrogels: Natural, biodegradable tissue engineering scaffolds. Biotech Bioeng 2003;82:578–89.

20. Nettles DL, Vail TP, Morgan MT, Grinstaff MW, Setton LA. Photocrosslinkable hyaluronan as a scaffold for articular cartilage repair. Ann Biomed Eng 2004;32:391–7. [PubMed: 15095813]

21. Ding S, Radosz M, Shen Y. Atom transfer radical polymerization of N, N-dimethylacrylamide. Macromol Rapid Commun 2004;25:632–6.

22. Abraham GA, de Queiroz AAA, Roman JS. Hydrophilic hybrid IPNs of segmented polyurethanes and copolymers of vinylpyrrolidone for applications in medicine. Biomaterials 2001;22:1971–85. [PubMed: 11426875]

23. Santos WLF, Porto MF, Muniz EC, Olenka L, Baessso ML, Bento AC, Rubira AF. Poly(ethylene terephtalate) films modified with N, N'-Dimethylacrylamide: Incorporation of disperse dye. J Appl Polym Sci 2000;77:269–82.

24. Whittaker P, Kloner RA, Boughner DR, Pickering JG. Quantitative assessment of myocardial collagen with picrosirius red staining and circularized light. Basic Res Cardiol 1994;89:397–410. [PubMed: 7535519]

25. Bromberg L, Grosberg AY, Matsuo ES, Suzuki Y, Tanaka T. Dependency of swelling on the length of subchain in poly (N, N-dimethylacrylamide)-based gels. J Chem Phys 1997;106:2906–10.

26. Haraguchi K, Farnworth R, Ohbayashi A, Takehisa T. Compositional effects on mechanical properties of nanocomposite hydrogels composed of poly (N, N-dimethylacrylamide) and clay. Macromolecules 2003;36:5732–41.

27. Baker JP, Hong LH, Blanch HW, Prausnitz JM. Effect of initial total monomer concentration on the swelling behavior of cationic acrylamide-based hydrogels. Macromolecules 1994;27:1446–54.

28. Ferrira L, Vidal MM, Geraldes CFGC, Gil MH. Preparation and characterization of gels based on sucrose modified with glycidyl methacrylate. Carbohydr Polym 2000;41:15–24.

29. Gong JP, Katsuyama Y, Kurokawa T, Osada Y. Double network hydrogels with extremely high mechanical strength. Adv Mater 2003;15:1155–8.

30. Koneko D, Tada T, Kurokawa T, Gong JP, Osada Y. Mechanically strong hydrogels with ultra-low frictional coefficients. Adv Mater 2005;17:535–8.

31. Flory, PJ. Principles of polymer chemistry. Cornell University Press; New York: 1953. Chapter XI

32. Hornebeck W. Down-regulation of tissue inhibitor of matrix metalloprotease-1 (TIMP-1) in aged human skin contributes to matrix degradation and impaired cell growth and survival. Pathol Biol (Paris) 2003;51:569–73. [PubMed: 14622947]

33. Rokhade AP, Shelke NB, Patil SA, Aminabhavi TM. Novel interpenetrating polymer network microspheres of chitosan and methylcellulose for controlled release of theophylline. Carbohydr Polym 2007;69:678–87.

34. Park YD, Tirelli N, Hubbell JA. Photopolymerized hyaluronic acid-based hydrogels and interpenetrating networks. Biomaterials 2003;24:893–900. [PubMed: 12504509]

35. Tamada Y, Ikada Y. Fibroblast growth on polymer surfaces and biosynthesis of collagen. J Biomed Mater Res 2004;28:783–9. [PubMed: 8083246]

36. Ramamurthi A, Vesely I. Smooth muscle cell adhesion on crosslinked hyaluronan gels. J Biomed Mater Res 2002;60:196–205.

37. Van der Valk P, Van Pelt AWJ, Busscher HJ, de Jong HP, Wildevuur CRH, Arends J. Interaction of fibroblast and polymer surfaces: Relationship between surface free energy and fibroblast spreading. J Biomed Res 1983;17:807–17.

38. Hallab NJ, Bundy KJ, O'connor K, Moses RL, Jacobs JJ. Evaluation of metallic and polymeric biomaterial surface, energy and surface roughness characteristics for directed cell adhesion. Tissue Eng 2001;7:55–71. [PubMed: 11224924]

39. Hoshiba T, Cho CS, Murakawa A, Okahata Y, Akaike T. The effect of natural extracellular matrix deposited on synthetic polymers on cultured primary hepatocytes. Biomaterials 2006;27:4519–28. [PubMed: 16697038]

40. Junqueira LCU, Bignolas G, Brentani RR. Picrosirius plus polarization microscopy, a specific method for collagen detection in tissue sections. Histochem J 1979;11:447–55. [PubMed: 91593]
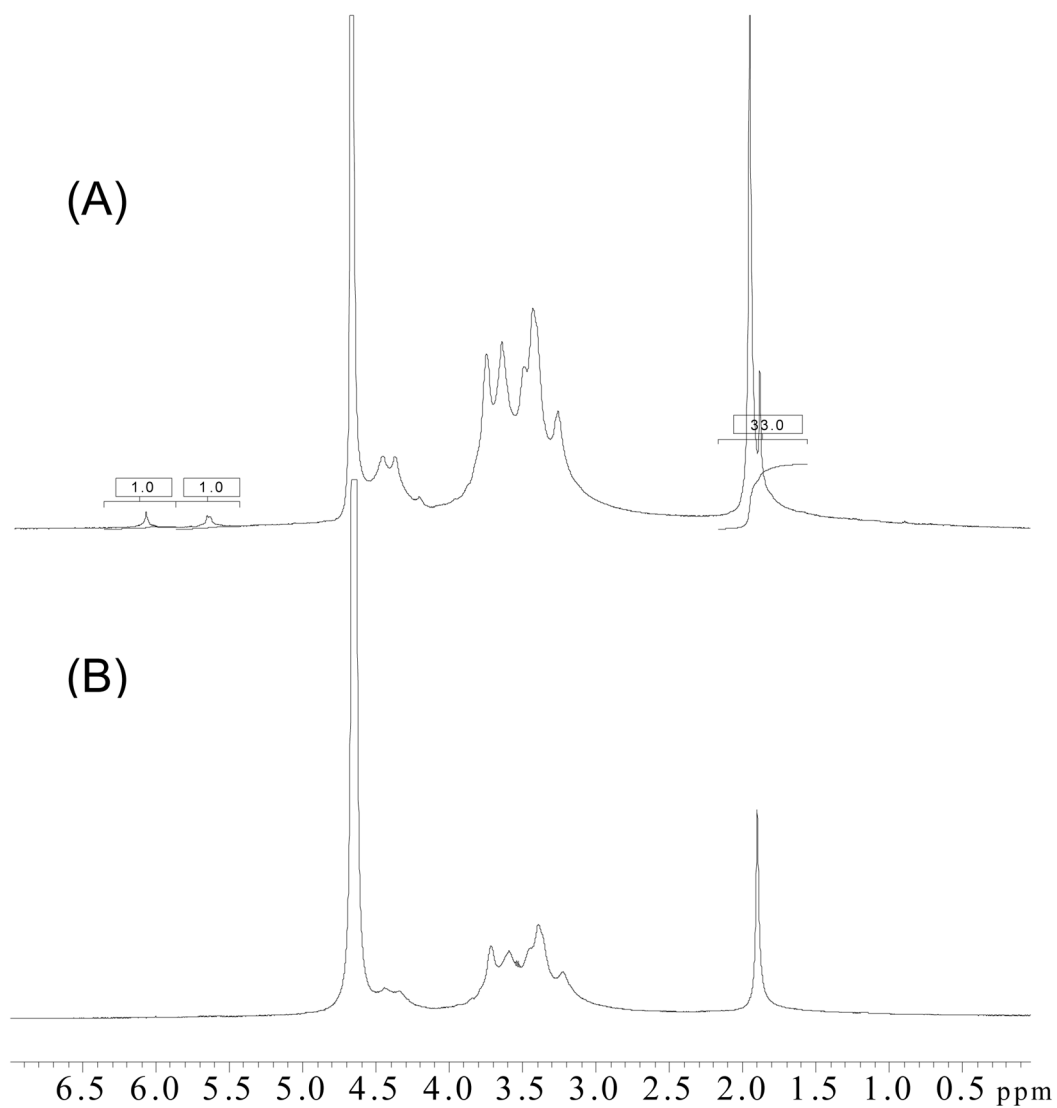
Fig. 1.
^{1}H NMR spectra of modified HA (A) and HA (B). The integrals in the boxes at 5.6, 6.1 and 1.9 ppm were 1.0, 1.0, and 33.0, respectively.
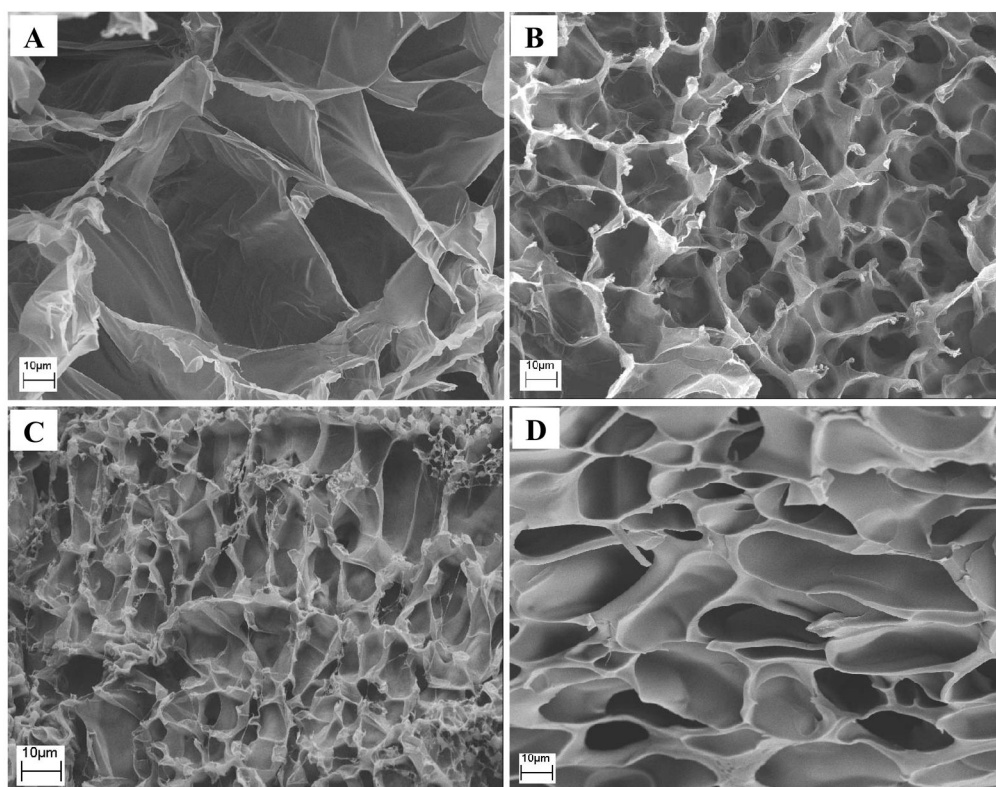
Fig. 2.
Representative SEM images for the PHA (A), PHA/D-3-0.01 (B), PHA/D-3-0.05(C), and PHA/D-3-2 (D) hydrogels. Scale bar: 10 µm.
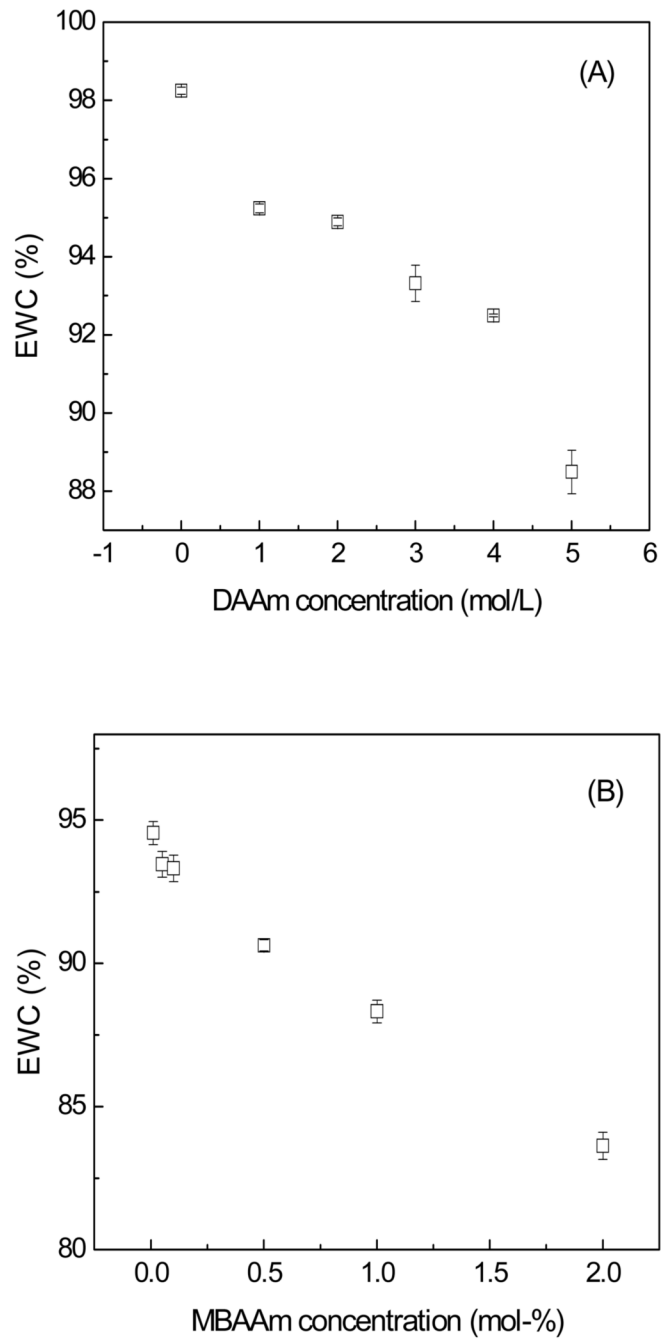
Fig. 3.
Variation of EWC for the hydrogels as a function of monomer (A) and crosslinker (B) of the second network.
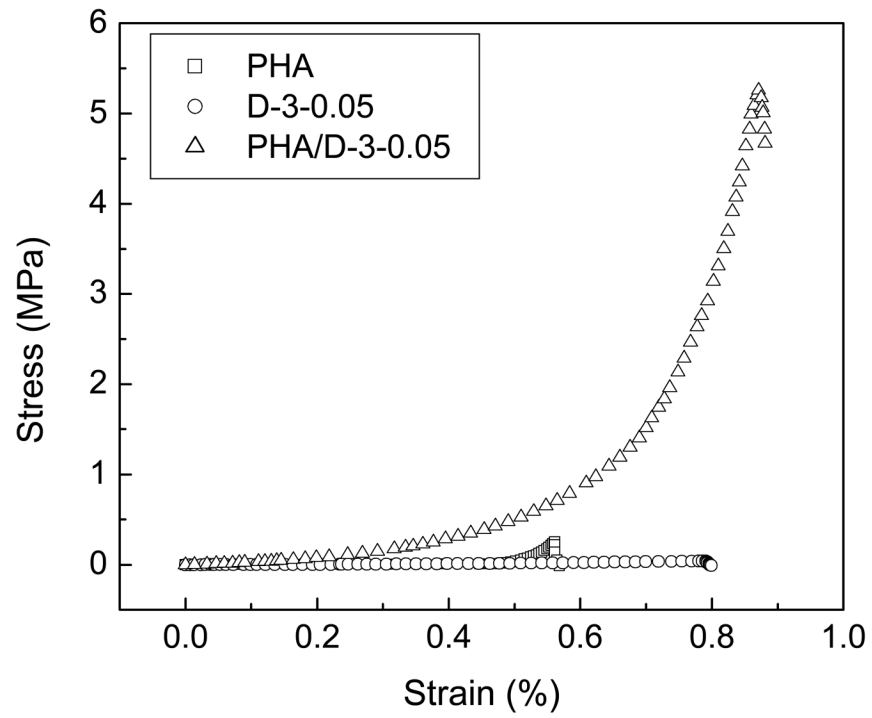
Fig. 4.
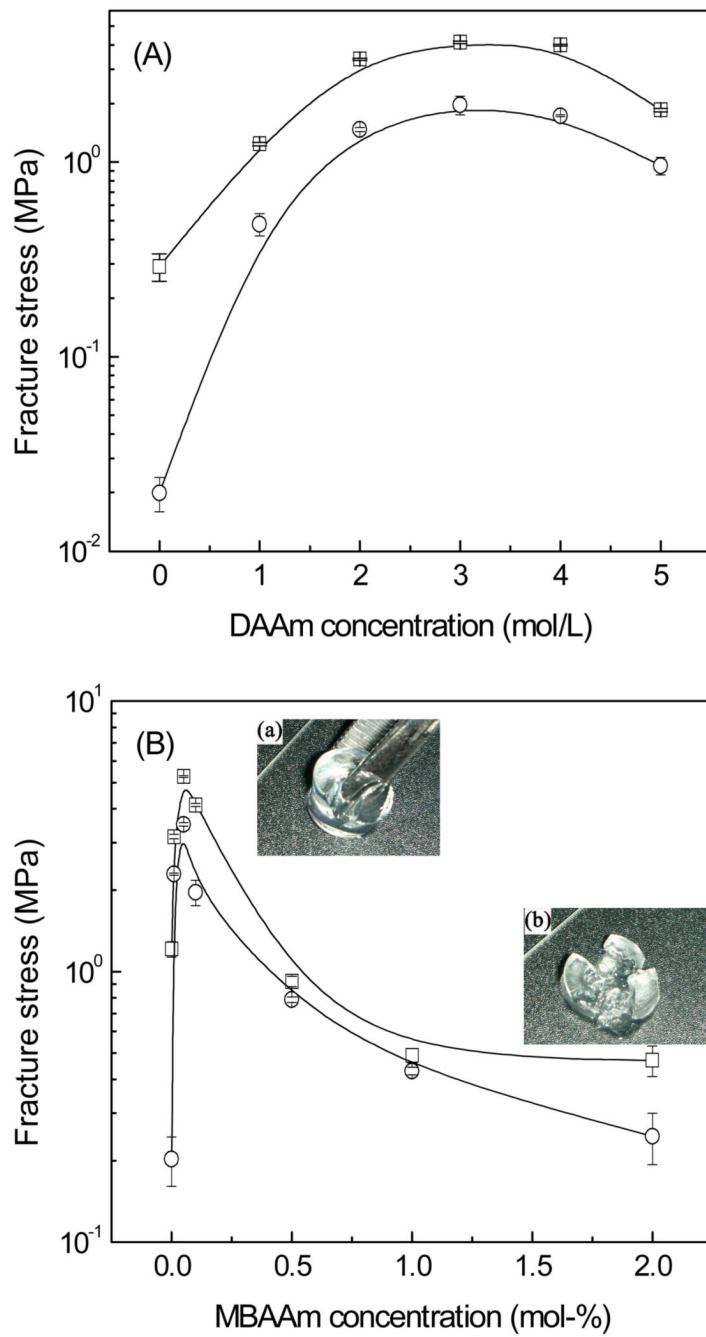Stress-strain profiles for the PHA, PHA/D-3-0.05 and P-3-0.05 hydrogels under uninaxial compression.

Fig. 5.
Dependence of the fracture stress of the hydrogels on the monomer concentration (A), and the crosslinker concentration (B), before (square) and after cell culture (circle).
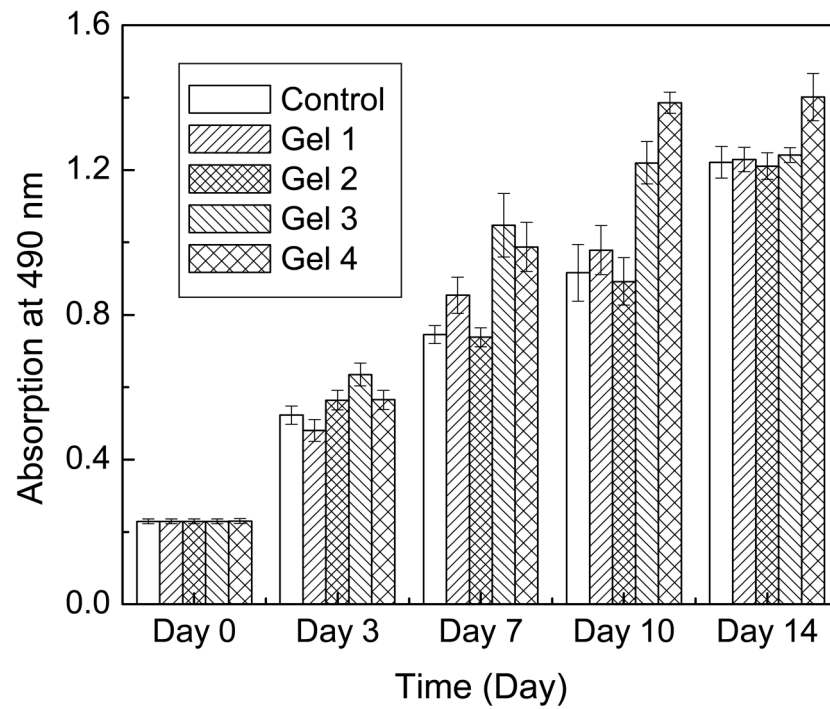
Fig. 6.
MTS assay of the cell viability with PHA/DAAm hydrogels. Gel 1: PHA/D-3-0.01; Gel 2: PHA/D-3-2; Gel 3: PHA/D-3-2; Gel 4: PHA compared to monolayer cells control by the indirect contact method.
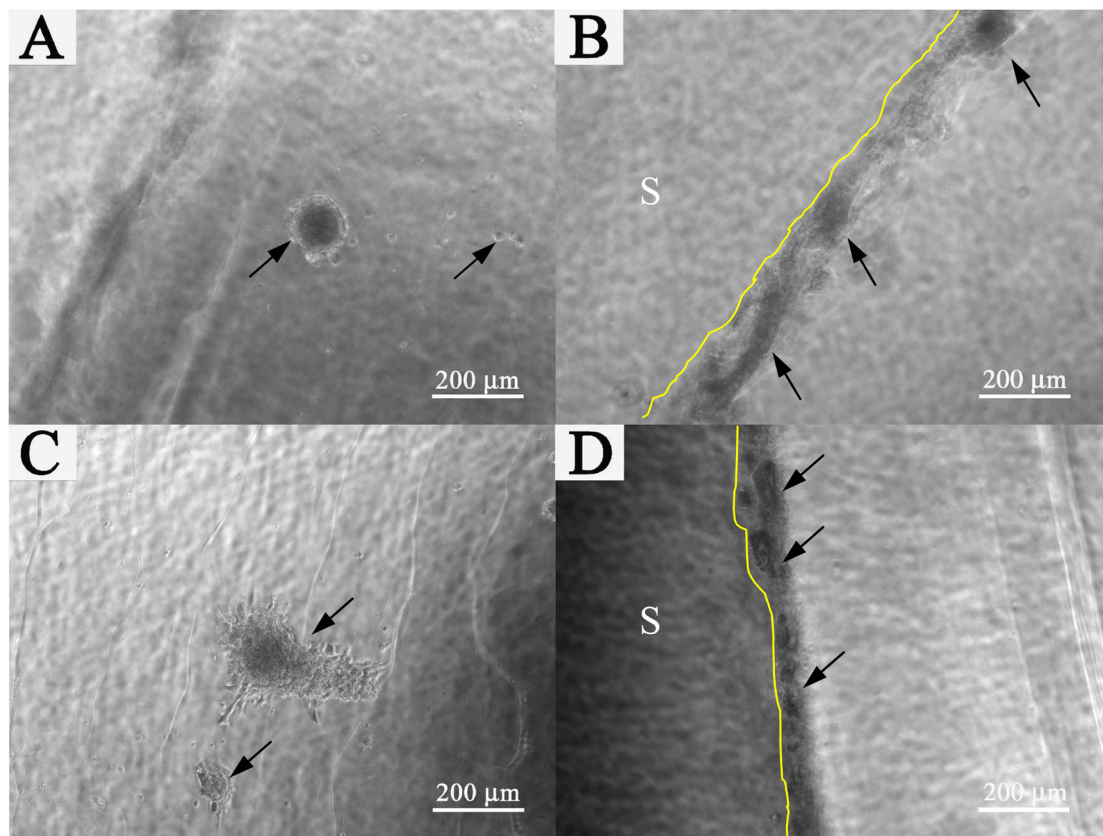
Fig. 7.
Cells on the surface and en face side of the hydrogels. (A) and (B) PHA/D-3-0.01, (C) and (D) PHA/D-3-0.05. (A), and (C): surfaces of hydrogels. (B) and (D): en face sides of hydrogels. **S**: Surface of hydrogels. ↟: Cell clusters on the surfaces or en face sides of hydrogels. Scale bar: 200 μm.
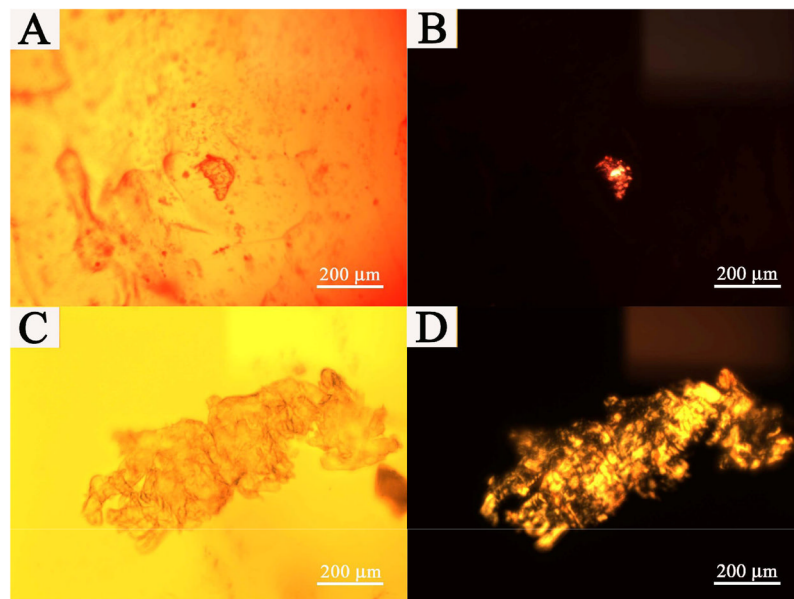
Fig. 8.
Collagen deposited on the hydrogel surfaces. Sirius Red staining. (A) and (B): PHA/D-3-0.01 hydrogel; (C) and (D): PHA/D-3-0.05 hydrogel. (A) and (C): conventional bright field images of hydrogel surfaces. (B) and (D): collagen on the hydrogel surfaces through polarization microscopy. Scale bar: 200 μm.
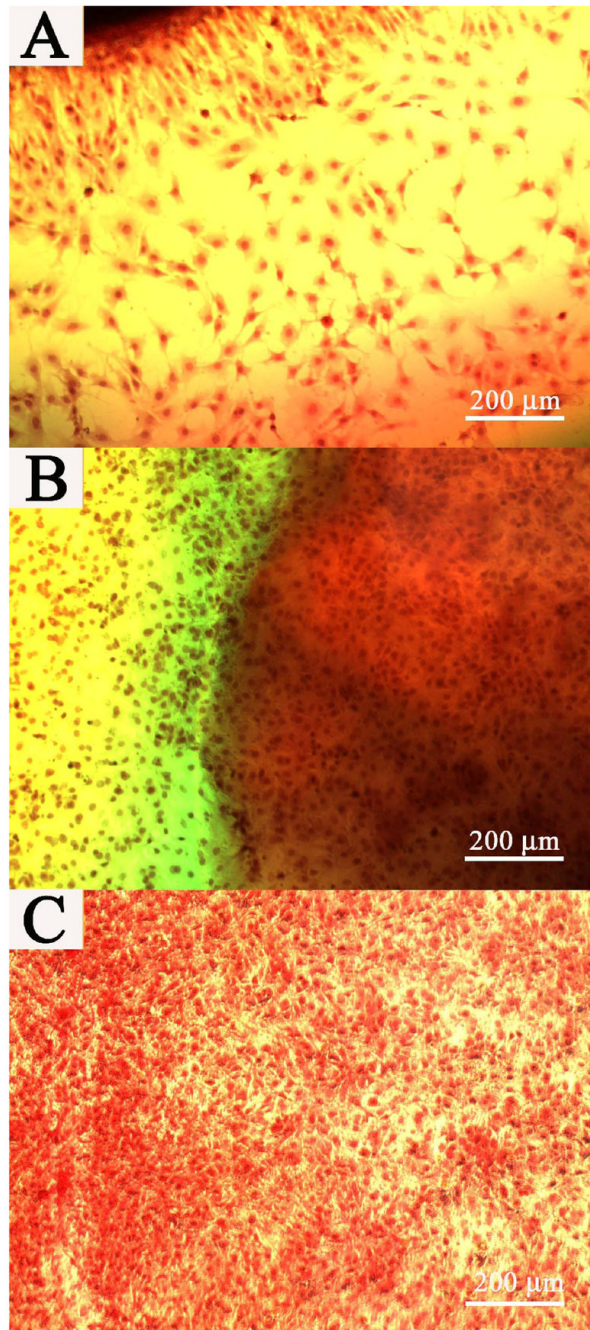
Fig. 9.
Cells on the well bottom and underneath the PHA/D-3-0.05 hydrogel after 1 week (A), 2 week (B), and 1 month cell culture(C). Image (B) was captured without removing the hydrogel. Scale bar: 200 μm.
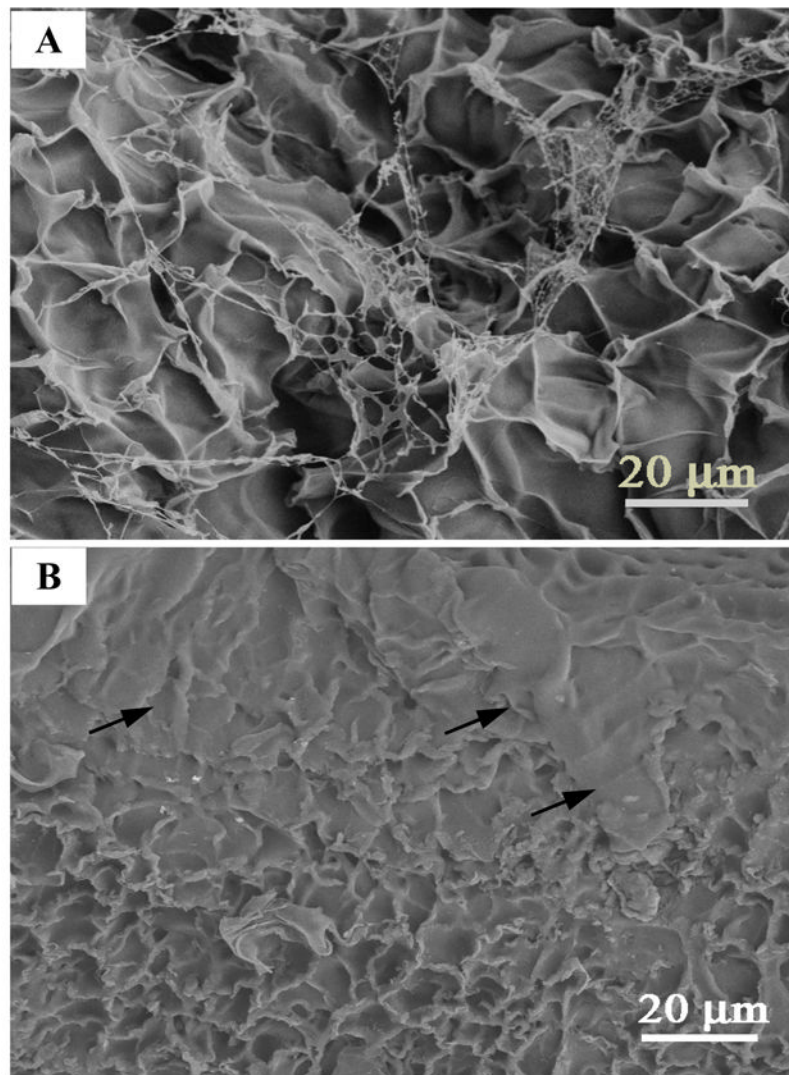
Fig. 10.
Representative SEM images for ECM deposition on the surface of the PHA/D-3-0.05 hydrogels. (A): the surface of the hydrogel without co-culturing with cells. (B): the surfaces of hydrogels co-cultured with cells for one month. ♠: Extracellular matrix. Scale bar: 20 μm.

Table 1

Representative results of the initial compressive moduli of the PHA/DAAm hydrogels before and after cell culture.

Elastic modulus (MPa)	PHA	PHA/D-3-0.01	PHA/D-3-0.05	PHA/D-3-2
Before cell culture	0.045±0.005	0.397±0.07	0.508±0.08	0.442±0.11
After cell culture	0.037±0.006	0.260±0.06	0.246±0.03	0.235±0.05